Eur. Phys. J. D **3**, 53–66 (1998)

THE EUROPEAN PHYSICAL JOURNAL D

Molecular photodynamics involved in multi-photon excitation fluorescence microscopy

J. Mertz[a]

School of Applied and Engineering Physics, Cornell University, Ithaca, New York, 14853, USA

Received: 9 March 1998 / Accepted: 20 April 1998

Abstract. We present a simple model for calculating the fluorescence generated by the multi-photon excitation (MPE) of molecules in solution. The model takes into account internal molecular dynamics such as ground-state depletion due to inter-system crossing (ISC), as well as external molecular dynamics associated with diffusion into and out of an excitation volume confined in 3-dimensions. Internal and external molecular dynamics are combined by using a technique of linearization of a modified diffusion equation which takes into account the possibility of concentration depletion due to photobleaching. In addition, we discuss the phenomenon of pulse saturation which effectively limits the molecular excitation rate constant in the case of short pulsed excitation. Our results are specifically applied in the context of fluorescence autocorrelation functions and single-molecule detection. In the latter case, we discuss some consequences of high-order multi-photon photobleaching. Finally, we include three appendices to rigorously define the temporal and spatial profiles of an arbitrary excitation beam, and also to discuss some properties of an exact evaluation of concentration depletion due to photobleaching.

PACS. 32.80.Wr Other multiphoton processes – 32.50.+d Fluorescence, phosphorescence (including quenching) – 87.64.-t Spectroscopic and microscopic techniques in biophysics and medical physics

1 Introduction

The quality of an image obtained with a fluorescence microscope is almost always limited by the quantity of fluorescence that is collected and processed to generate the image. It is therefore important to thoroughly understand the physical processes limiting this fluorescence. Until recently, most fluorescence microscopes have operated under the principle of one photon excitation (1PE), whereby a single excitation photon from a laser or from a lamp is sufficient to excite a fluorescent molecule [1]. With the invention of nonlinear microscopy, this principle has been extended to two-photon excitation (2PE) [2,3], followed by three-photon excitation (3PE) [4–6], opening the door to fluorescence imaging *via* multi-photon excitation (MPE) [4], whereby more than one photon are required to excite a fluorescent molecule. In practice, the illumination beam is generally a continuous wave (CW) for 1PE, whereas the illumination laser beam must be pulsed for MPE, owing to the large photon densities required to generate an adequate amount of fluorescence.

A fundamental advantage of MPE microscopy over conventional (1PE) widefield or confocal microscopy is that MPE is inherently confined to a small volume in 3-dimensions [2,7,8], and hence occasions little damage to the sample or to fluorescent molecules outside the volume. In other words, only those molecules that are imaged (*i.e.* those molecules that fluoresce from within the excitation volume) are subjected to photodamage, whereas in conventional confocal microscopy many molecules are subjected to photodamage that are never imaged. This advantage has been demonstrated, for example, in the deep imaging of fluorescent species in highly turbid media such brain tissue [9,10], and in the imaging of fragile molecules such as autofluorescent proteins [4,11–13] or amino-acids or cell messengers [14,15].

The purpose of this article is to detail the physical processes that limit the amount of fluorescence emitted by one or more molecules undergoing MPE in a solvent. Particular care is taken to distinguish the effects of pulsed illumination as compared to CW illumination, since the former is almost always required in MPE and can have significant consequences on both the excitation rate constant and volume. These consequences can play a role, for example, when dealing with fluorescence correlation spectroscopy (FCS) [16–19], fluorescence photobleaching recovery (FPR) [20], or uncaging [21,22]. We derive simple expressions for ground state depletion and saturation, both of which limit the rate at which a molecule can fluoresce. In addition, we present various scenarios taking into account the possibility of photodamage, which limits the total amount of fluorescence that can be emitted by

[a] *present address*: Laboratoire de Physiologie, École Supérieure de Physique et Chimie Industrielle, 75005 Paris, France.
e-mail: mertz@atlas.bio.espci.fr

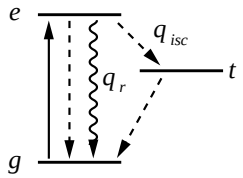

Fig. 1. Simple model of a molecule consisting of a ground state g and an excited state e from which the molecule can fluoresce with a quantum yield q_r or non-radiatively decay to the lowest level triplet state t with a quantum yield q_{isc}.

a molecule. When imaging fluorescent molecules, a reduction in fluorescence rate can be compensated, whenever practical, by an increase in the time allotted for an image acquisition. On the other hand, a limitation in the total amount of fluorescence cannot be compensated. As such, photodamage is almost always the predominant factor limiting image quality in fluorescence microscopy.

We close this article by noting that in some cases MPE does not always present an advantage over 1PE. In regimes where a high order fluorescence excitation process occasions a higher order photodamage process (for example, if 2PE fluorescence occasions 3PE photodamage) then the curtailing of fluorescence due to photodamage may be so severe that the advantages of the high order fluorescence excitation are outweighed. This phenomenon is considered in the specific example of single-molecule 2PE fluorescence detection, and is speculated to account for the deficiencies in reported signals [23–25].

The global layout of the article is divided into three parts. The first part is limited to a discussion of molecular fluorescence in "closed" systems, that is, systems in which only the internal dynamics of molecules play a role since the molecules are regarded as effectively isolated from an outside world. The second part is limited to a discussion of molecular fluorescence in "open" systems in which the internal dynamics of molecules are neglected and instead only their external dynamics are considered. Finally, the third part combines the results for "closed" and "open" system dynamics through a technique of linearization, with particular emphasis both on fluorescence autocorrelation functions and single molecule detection. In general, we try to simplify our formalism as much as possible in order to distill the basic principles involved and cast our results in forms amenable to "back-of-the-envelope" calculations.

2 Average fluorescence rate

We first consider only the simplest model of a molecule which illustrates most of the key processes governing fluorescence (see Fig. 1). For a molecule to fluoresce, it must be excited. At any given instant τ, the excitation rate of the molecule, defined as the probability that the molecule is excited per unit time, is given by $g(\tau)\alpha(\tau)$, where $g(\tau)$ is the instantaneous probability that the molecule is in the ground state, and $\alpha(\tau)$ is the instantaneous excitation rate constant, governed by the excitation light intensity and the molecular absorption cross-section.

In deriving the resultant averaged fluorescence rate, we consider the cases of CW and pulsed excitation separately. In the case of CW excitation, α is a bona fide constant, and hence the average fluorescence rate is given simply by

$$\overline{f} = q_r \overline{g}\ \overline{\alpha}, \tag{1}$$

where q_r is the radiative quantum yield which, in general, depends on the solvent (an overstrike denotes a time average).

In the case of pulsed excitation, the situation is somewhat more complicated and one must first consider the average amount of fluorescence generated per excitation pulse. To this end, we make the following assumptions which are used throughout this paper: i) the duration τ_p of each pulse is considerably shorter than the molecule's excited state lifetime τ_e, and ii) the interval τ_l between pulses is considerably longer than the molecule's excited state lifetime. In practice, the most commonly used illumination source for MPE is a mode-locked Ti:Sapphire laser for which $\tau_p \approx 100$ fs and $\tau_l \approx 10$ ns. Inasmuch as molecular excited state lifetimes are typically on the order of a few nanoseconds, assumption (i) is entirely justified whereas assumption (ii) is reasonably justified. An important consequence of assumption (i) is that a molecule can be excited effectively no more than once per pulse. We derive this by noting that the probability that a molecule is excited more than once per pulse becomes independent of α for large α and is no larger than of order τ_p/τ_e, which is negligibly small here ($< 10^{-4}$). The ramifications of this deceptively simple consequence will be discussed at length in Section 6.

Denoting ξ (between 0 and 1) as the probability that a molecule is excited during a pulse given that the molecule definitely starts in the ground state at the onset of the pulse, then the average fluorescence rate of the molecule becomes simply $\overline{f} = q_r \overline{g}\, \overline{\alpha}$, with the prescription here that g is sampled only at the *onset* of each pulse and that $\overline{\alpha} = \xi/\tau_l$. In other words, $\overline{f}$ can be expressed in the same form (Eq. (1)) for both CW and pulsed excitation. We note that $\overline{g}$ depends on the internal state of the molecule whereas $\overline{\alpha}$ is independent of the internal state of the molecule.

3 Ground-state depletion

It is clear that any reduction in $\overline{g}$, known as a ground-state depletion, will lead to a reduction in the average fluorescence rate of the molecule. Several factors can contribute to ground state depletion. We will first discuss those governed by the molecule's internal dynamics and defer those governed by the molecule's external dynamics to Section 4.

Referring to the model in Figure 1, the rate equations governing a molecule's internal dynamics can be written

in simple matrix form:

$$\frac{d}{d\tau}\begin{pmatrix} g \\ e \\ t \end{pmatrix} = \begin{bmatrix} -\alpha & (1-q_{isc})/\tau_e & 1/\tau_t \\ \alpha & -1/\tau_e & 0 \\ 0 & q_{isc}/\tau_e & -1/\tau_t \end{bmatrix} \begin{pmatrix} g \\ e \\ t \end{pmatrix} \equiv \mathbf{M} \begin{pmatrix} g \\ e \\ t \end{pmatrix} \quad (2)$$

where the generalization to a more complicated level system is straightforward. The steady-state solution for g in the case of CW excitation is given by

$$\overline{g} = \frac{1}{1+\overline{\alpha}(\tau_e + q_{isc}\tau_t)} \,. \quad (3)$$

In the case of pulsed excitation, again following the prescription that g, e, and t are sampled only at the onset of each pulse, the rate equations reduce to those of a two-level system ($e \cong 0$), and the solution is simply

$$\overline{g} = \frac{1}{1+\overline{\alpha} q_{isc}\tau_t} \,. \quad (4)$$

In both cases, g decreases with increasing α. The onset of ground-state depletion for CW excitation occurs when $\overline{\alpha} \approx 1/(\tau_e + q_{isc}\tau_t)$, whereas for pulsed excitation it occurs when $\overline{\alpha} \approx 1/q_{isc}\tau_t$. For popular dye molecules such as fluorescein or rhodamine, the quantities τ_e and $q_{isc}\tau_t$ are typically of the same order of magnitude, meaning that the onset of ground-state depletion occurs when these molecules are excited at about the same rate as they can fluoresce (> 100 MHz). We point out that such an average excitation rate can only barely be approached with current mode-locked Ti:Sapphire lasers.

Referring to equation (1), the onset of ground-state depletion means that $\overline{f}$ no longer scales linearly with $\overline{\alpha}$, though it continues to monotonically increase with $\overline{\alpha}$. We emphasize here that we have not yet specified the dependence of $\overline{\alpha}$ on the illumination intensity (for example this could be power squared for 2PE, power cubed for 3PE, *etc.*). As such, $\overline{\alpha}$ should be interpreted as a generalized excitation rate.

Finally, we point out that the phenomenon of ground-state depletion is often referred to in the literature as "saturation". In keeping with our definition of g for pulsed excitation, ground- state depletion in this paper is interpreted as being relatively long-lived in that its effect can subsist from pulse to pulse. We reserve the term "saturation" for the effect of intra-pulse ground- state depletion only (see Sect. 6).

4 Diffusion and photobleaching

In our analysis of the internal dynamics of a molecule, we have tacitly assumed that the molecule is in closed system, that is, that the molecule must reside in only states g, e or t (*i.e.* $\det[\mathbf{M}]=0$) and that the molecule can be excited regardless of its external dynamics (*e.g.* location in space). In practice, however, the volume V in which a molecule can be excited is usually much smaller than the sample volume containing the molecule, meaning that a molecule which is being excited can simply diffuse out of V, effectively curtailing the possibility of its being further excited. Moreover, mechanisms other than diffusion can cause a molecule to "exit" V. In particular, an excited molecule can undergo photobleaching, defined here as a photo-chemical reaction that permanently removes the molecule from the excitation-fluorescence cycle. As pointed out in the introduction, photobleaching ultimately limits the quality of imaging in fluorescence microscopy, and its effects cannot be neglected.

As opposed to Section 3 where we examined only the internal dynamics of a molecule in a closed-system, we will examine here only the external dynamics of a molecule in an open-system. That is, we will consider here only the effects of diffusion and photobleaching. A more complete picture of molecular dynamics is deferred to Section 5.

To begin, let us denote q_b as a phenomenological quantum yield for photobleaching, assumed a constant. In other words, every time a molecule is excited, it has a probability q_b of being photobleached. Because we are only considering external dynamics here, a molecule (or population of molecules) is completely described by a local concentration distribution $C(r,z,\tau)$, where r and z are radial and axial coordinates relative to the focal center of the illumination beam (see Appendix B), and the dimension of C is number-of-molecules/unit-volume. The evolution of C is described by

$$\frac{\partial}{\partial\tau}C(r,z,\tau) = D\nabla^2 C(r,z,\tau) - q_b\overline{\alpha}(r,z)C(r,z,\tau) \quad (5)$$

where the first term on the right dictates the evolution of C governed by diffusion (D is the molecule's diffusion constant), and the second term on the right dictates the evolution of C governed by photobleaching. We have assumed that diffusion and photobleaching are slow relative to the pulse repetition rate (in the case of pulsed excitation), and we have made explicit the spatial dependence of α which is defined by the illumination beam profile (given by $W(r,z)$; see Appendix B).

Equation (5) represents a partial differential equation which, in general, must be solved numerically. In particular, we are interested here in the steady-state solution for C. Two cases must be distinguished. In the case of 1PE, typically V is bounded radially by a Gaussian illumination beam profile, and axially by the walls of the sample container. As such, the diffusion into and out of V is effectively restricted to 2 dimensions, meaning that C will continually deplete with time and never reach a steady state. In other words, the diffusion of new molecules into V is too slow to counterbalance the removal of molecules from V due to photobleaching, no matter how small q_b. In the case of MPE, V is defined by the illumination beam profile alone and is almost always much smaller than the sample volume. Diffusion into and out of V then takes place in 3 dimensions and the depletion of C by photobleaching can be counterbalanced by the diffusion of fresh

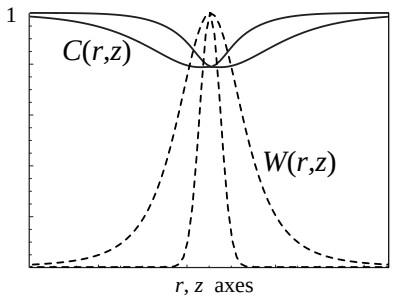

Fig. 2. Example of the steady-state concentration $\overline{C}(r,z)$ for the case of 2PE photobleaching with a Gaussian-Lorentzian excitation profile ($z_0/w_r = 2.5$), such that $a = D/q_b w_r^2$. Only profiles along the r-axis (narrow curves) and the z-axis (wide curves) are shown. $\overline{C}(r,z)$ is normalized to the concentration C_∞ far from the focal center. $W(r,z)$ equals $\overline{\alpha}(r,z)/\overline{\alpha}(0,0)$.

molecules into V, no matter how large q_b. In other words, given time, C eventually reaches a steady state. A steady-state solution to equation (5) obtained numerically using the relaxation method [26] is presented in Figure 2. We note that the profile of the depletion in $\overline{C}$ is broader than that of α. This is a general result which is independent of the magnitude of α (see Appendix C).

The total fluorescence rate obtained from a population of molecules is given by the volume integral (neglecting internal dynamics):

$$\overline{F} = q_r \int \overline{\alpha}(r,z)\overline{C}(r,z)dv. \tag{6}$$

When there is no photobleaching, then $\overline{C}(r,z) = C_\infty$ and $\overline{F}$ is linearly dependent on $\int \overline{\alpha}$. When photobleaching is sufficient to begin depleting $C(r,z)$, then $\overline{F}$ deviates from its linear dependence on $\int \overline{\alpha}$.

Though equation (5) constitutes an exact formulation of the dynamics of a molecule governed by diffusion and photobleaching, it is both tedious and time consuming to solve and hence it is of little practical use. In particular, if one generalizes equation (5) to include the internal dynamics of molecules as described in Section 3, then solutions become intractable and a simpler formulation of the problem is highly desirable. To this end, we define C_{in} as the average concentration inside the excitation volume V, that is,

$$C_{in} = \frac{1}{V}\int_V \overline{C}(r,z)dv. \tag{7}$$

Using Green's theorem, and assuming that C is relatively flat under the illumination beam profile (see Appendix C), we can then approximate equation (5) by the simpler equation

$$\frac{\partial}{\partial\tau}C_{in} \approx (C_\infty - C_{in})/\tau_d - q_b\langle\overline{\alpha}\rangle C_{in} \tag{8}$$

where $\langle\overline{\alpha}\rangle$ represents a spatial average of $\overline{\alpha}$ over V, and τ_d represents the average dwell time of a molecule in V. We

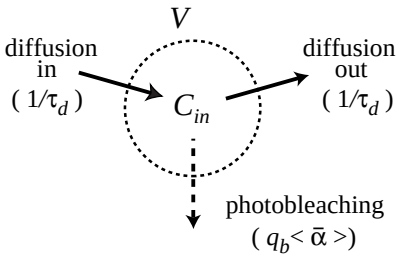

Fig. 3. Simple model of open-system dynamics. Fresh molecules diffuse into the excitation volume V with rate constant $1/\tau_d$. Molecules exit V either by diffusion with rate constant $1/\tau_d$, or by photobleaching with rate constant $q_b\langle\overline{\alpha}\rangle$. The resultant average concentration in V is C_{in}.

define dwell time here as the time interval between when a molecule first enters V and last exits V, given by

$$\tau_d = \frac{V}{J_{in}}C_\infty \tag{9}$$

where J_{in} represents the flux of molecules entering V for the first time. As a simple illustrative example, we consider a hard-sphere excitation volume of radius r_0 (see Appendix C). In this case, $J_{in} = 4\pi r_0 D C_\infty$ [27] and hence $\tau_d = r_0^2/3D$. In the more realistic case where the excitation volume profile is diffuse, then J_{in} is more difficult to define and τ_d must be estimated, as is done below.

The physical interpretation of equation (8) is described in Figure 3. Molecules can freely diffuse into and out of the excitation volume with a rate constant τ_d^{-1}, however once in the volume they can also be photobleached with a rate constant $q_b\langle\overline{\alpha}\rangle$. The ratio R of the average emitted fluorescence including the possibility of photobleaching to the average emitted fluorescence excluding the possibility of photobleaching is then approximated by, following equation (8),

$$R \approx \frac{C_{in}}{C_\infty} \approx \frac{1}{1 + \langle\overline{\alpha}\rangle q_b \tau_d}\,. \tag{10}$$

Further approximations can be made to quantify $\langle\overline{\alpha}\rangle$ and τ_d. In particular, $\langle\overline{\alpha}\rangle$ can be approximated as the average of $\overline{\alpha}$ over excited molecules, that is $\langle\overline{\alpha}\rangle \cong \gamma a$, where γ is the volume contrast of the excitation profile and $a = \overline{\alpha}(0,0)$ (see Appendix B), and τ_d can be approximated by fitting equation (10) to a numerical evaluation of R obtained from equation (5). We find for different 2PE excitation profiles, and assuming the relation $w_z^2, z_0^2 \gg w_r^2$ which is always the case in practice (see Appendix B for definitions of w_r, w_z, and z_0):

$$\tau_d \approx \frac{w_r^2}{2.5D}\ln\left(2\frac{w_z}{w_r}\right) \quad \text{(Gaussian ellipsoid)} \tag{11}$$

$$\tau_d \approx \frac{w_r^2}{1.8D}\ln\left(6\frac{z_0}{w_r}\right) \quad \text{(Gaussian} - \text{Lorentzian)} \tag{12}$$

A comparison between R as obtained from equation (10) and R as obtained fully numerically from equation (5) is illustrated in Figure 4. Considering the simplicity of

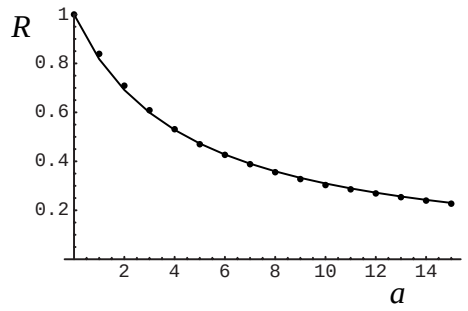

Fig. 4. Fluorescence generated by a solution of molecules excited by 2PE with a Gaussian-ellipsoidal profile ($w_z/w_r = 2.5$). R is the ratio of total fluorescence with photobleaching to total fluorescence without photobleaching. The excitation amplitude a is expressed in units $D/q_b w_r^2$.

equation (10), its apparent accuracy is notable. We emphasize that the same level of accuracy is typical for a wide variety of different excitation profile parameters.

Referring to equation (10), we note that a reduction in fluorescence due to concentration depletion caused by photobleaching occurs when $\langle\overline{\alpha}\rangle q_b \tau_d \gg 1$. Since the logarithmic factors in equations (11) and (12) vary slowly with changes in the illumination profile, we may consider τ_d as roughly proportional to w_r^2. Recalling that the illumination intensity I scales as w_r^{-2}, we observe that in the case of MPE ($\alpha \propto I^2$, I^3, *etc.*), an increase in w_r can significantly alleviate the problem of photobleaching depletion.

5 Fluorescence autocorrelation

At this point, we may combine the internal closed-system dynamics of a molecule, as described by equation (2), with the open-system dynamics described in their simplified form by equation (8) in order to obtain a more complete picture of molecular fluorescence. Because both equations are linear, their combination is straightforward. For convenience, we express our results in terms of numbers of molecules rather than concentrations. For example, we denote N_g as the number of molecules in V that are in the ground state (*etc.*). The full dynamics of the molecules in V are then given by

$$\frac{d}{d\tau}\begin{pmatrix} N_g \\ N_e \\ N_t \end{pmatrix} = \left(\mathbf{M} - \tau_d^{-1}\mathbf{I}\right)\begin{pmatrix} N_g \\ N_e \\ N_t \end{pmatrix} + \tau_d^{-1}\begin{pmatrix} \overline{N} \\ 0 \\ 0 \end{pmatrix} \qquad (13)$$

where again $\mathbf{M}$ is the matrix that describes the internal dynamics of the molecules, however here it can include the possibility of photobleaching, that is, $\det[\mathbf{M}]$ may or may not equal 0 (we will present various scenarios for photobleaching in Sect. 7). The second term on the right describes the diffusion of molecules out of V ($\mathbf{I}$ is the identity matrix). The third term on the right, or driving term, describes the diffusion of fresh molecules into V, which by definition are in the ground state since they are entering V for the first time. $\overline{N}$ here represents the average total number of molecules in V regardless of whether or not they are photobleached (*i.e.* $\overline{N} = C_\infty V$). We emphasize that, precisely because of photobleaching, $\overline{N}_g + \overline{N}_e + \overline{N}_t$ is not in general equal to $\overline{N}$.

The solution to equation (13) can be expressed in a variety of different manners. We choose here to express the solution in the context of the fluorescence autocorrelation function, since this is widely used to characterize both the internal and external dynamics of molecules [16–19], as well as to calibrate the excitation volume (see Appendix B). In its normalized form, the fluorescence autocorrelation function is defined by

$$G_F(\tau) = \frac{\overline{\delta F(t)\delta F(t+\tau)}}{\overline{F}^2} \qquad (14)$$

where $\delta F(t) = F(t) - \overline{F}$ represents the fluctuations in the total generated fluorescence, and the overstrike indicates a long time average over the variable t ($G(\tau)$'s with different subscripts throughout this article are defined similarly). If we assume, as is almost always the case in practice, that the decay rate constant from the excited state τ_e^{-1} is faster than all other relevant rate constants governing a molecule's dynamics (*e.g.* α, τ_t^{-1}, τ_d^{-1} *etc.*; see Appendix B), then for correlation times $\tau \gg \tau_e$ one obtains the simple relation $G_F(\tau) = G_{N_g}(\tau)$, which in turn may be re-expressed as

$$G_{N_g}(\tau) = \frac{\mathrm{Prob}[in, g; \tau]}{\overline{N}_g}\,. \qquad (15)$$

In the above expression, $\overline{N}_g$ denotes the steady-state solution to N_g obtained from equation (13), and $\mathrm{Prob}[in, g; \tau]$ denotes the probability that an individual molecule is both in the excitation volume and in the state g at time τ, given that it starts in the volume and in state g at time $\tau = 0$ (*i.e.*: $\mathrm{Prob}[in, g; 0] \equiv 1$). The molecules are assumed to be non-interacting, hence there is no correlation between different molecules.

An evaluation of $\mathrm{Prob}[in, g; \tau]$ is obtained from the homogeneous solution to equation (13), that is, the solution to equation (13) without the driving term. More specifically,

$$\mathrm{Prob}[in, g; \tau] = p_{in}(\tau) g(\tau) \qquad (16)$$

where $p_{in}(\tau)$ denotes the probability that the molecule is in V, without regard to its internal state or whether it is photobleached, and $g(\tau)$ now denotes the conditional probability that the molecule is in state g given that it is also in V, with initial conditions $p_{in}(0) = g(0) \equiv 1$. Separating equation (13) (without the driving term) into components operating on external and internal dynamics respectively, we arrive at the set of independent rate equations:

$$\frac{d}{d\tau} p_{in} = -\tau_d^{-1} p_{in} \qquad (17)$$

$$\frac{d}{d\tau}\begin{pmatrix} g \\ e \\ t \end{pmatrix} = \mathbf{M}\begin{pmatrix} g \\ e \\ t \end{pmatrix}. \qquad (18)$$

The solution to equation (17) is a simple exponential: $p_{in}(\tau) = e^{-\tau/\tau_d}$, whereas the solution to equation (18) depends on the particular internal dynamics of the molecule in question. For example, we consider the dynamics illustrated in Figure 1, to which we add the possibility of photobleaching either from state e with probability q_{eb} (meaning $q_b = q_{eb}$; see definition of q_b in Sect. 4), or from state t with probability q_{tb} (meaning $q_b = q_{isc}q_{tb}$). In the case of pulsed MPE and assuming for simplicity that $\tau_t \ll \tau_d$, we obtain

$$\overline{g} = \frac{\overline{N}_g}{\overline{N}} = \frac{1}{1 + \langle\overline{\alpha}\rangle(q_{isc}\tau_t + q_b\tau_d)} \cdot \tag{19}$$

Equation (19) represents the probability that a molecule in the excitation volume is also in the ground state. As expected, we observe that $\overline{g}$ behaves effectively as a combination of equations (4) and (10).

Having laid the necessary groundwork, we can now examine the MPE fluorescence autocorrelation function in detail. Let us first consider the scenario where either $\langle\overline{\alpha}\rangle$ is small, or where there is no ISC nor photobleaching ($q_{isc} = q_b = 0$). We then find $g(\tau) = 1$ and $G_F(\tau)$ is simply equal to $p_{in}(\tau)/\overline{N}$, as illustrated in Figure 5a. In this scenario, the average number of molecules in the excitation volume can be directly evaluated from the relation $G_F(0_+) = 1/\overline{N}$, and indeed this relation is used to define the excitation volume itself (see Appendix B; we use $\tau = 0_+$ here to indicate that we are still in the regime $\tau \gg \tau_e$). After a dwell time $\tau \approx \tau_d$, molecules in V eventually diffuse out of V, and $G_F(\tau)$ decays to zero.

If we now allow the possibility of ISC ($q_{isc} \neq 0$) while still disallowing the possibility of photobleaching ($q_b = 0$), then $G_F(\tau)$ takes on a different profile, as illustrated in Figure 5b. In particular, $G_F(0_+) = 1/\overline{N}_g$ meaning that, on average, only a fraction $\overline{g}$ of the molecules in V are fluorescing. The apparent shoulder in $G_F(\tau)$ may be interpreted as follows: those molecules that are not fluorescing at time $\tau = 0$ because they are in the triplet state eventually decay back to the ground state after a time $\tau \approx \overline{g}\tau_t$, whereupon they can re-enter the excitation-fluorescence cycle.

Finally, if $\langle\overline{\alpha}\rangle$ is sufficiently large and we allow the possibility of ISC and photobleaching ($q_{isc} \neq 0,\ q_b \neq 0$), then $G_F(0_+) = 1/\overline{N}_g$ can be much larger than $1/\overline{N}$, as illustrated in Figure 5c. Moreover, molecules may exit the excitation-fluorescence cycle *via* photobleaching as well as diffusion, meaning that the decay of $G_F(\tau)$ towards zero begins at an earlier time than τ_d. We denote this earlier time as τ_{eff}, corresponding to the average length of time a molecule can fluoresce in V, which is given by

$$\frac{\tau_{eff}}{\tau_d} = \frac{1}{1 + \langle\overline{\alpha}\rangle q_b\tau_d} \cdot \tag{20}$$

The above relation provides an alternative interpretation to equation (10).

The examples shown in Figures 5a-c illustrate that the effects of internal dynamics can be quite dramatic. In particular, molecules possessing no internal dynamics would exhibit no variations in $G_F(\tau)$ as a function of $\langle\overline{\alpha}\rangle$. Manifestly, this not the case when internal dynamics are included.

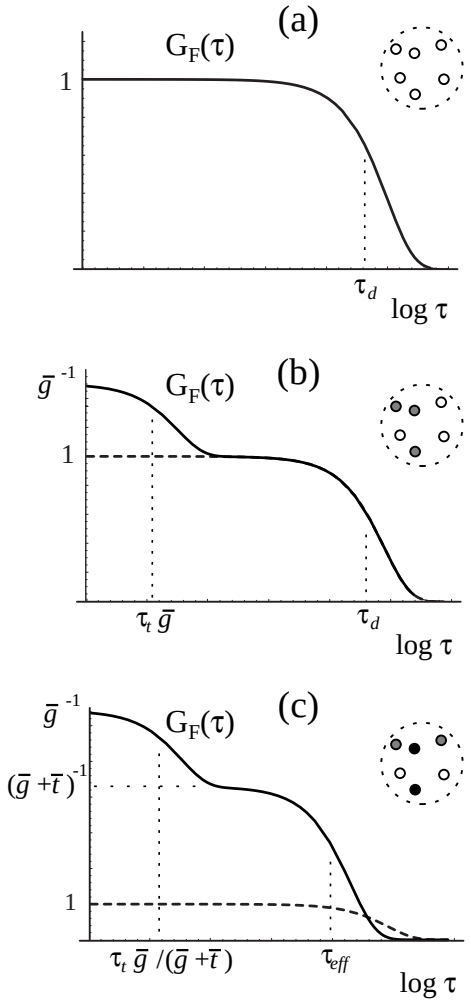

Fig. 5. Schematic examples of fluorescence autocorrelation functions when (a) all molecules are excitable at all times (white); (b) ISC is allowed and some molecules can temporarily reside in the triplet state (gray); (c) photobleaching is allowed and molecules can be permanently removed from excitation-fluorescence cycle (black). $G_F(\tau)$'s are normalized to $1/\overline{N}$, where $\overline{N}$ is the average number of molecules in the excitation volume. Assumptions for figures: $\tau_p \ll \tau_e \ll \tau_l \ll \tau_t \ll \tau_d$, and $q_{eb}, q_{tb} \ll q_{isc}$.

We close this section by noting that the simple form of $p_{in}(\tau)$ derived above (solution to Eq. (17)) is the result of our having reduced the exact diffusion dynamics governed by equation (5) to a single rate constant for diffusion into and out of V (see Fig. 3). A more accurate expression for $p_{in}(\tau)$ may be obtained from the full-blown solution to $G_F(\tau)$ given the particular excitation profile in question and assuming no internal dynamics. For example, in the case of 2PE, the full solution to $p_{in}(\tau)$ for a

Gaussian-ellipsoid excitation profile is given by

$$p_{in}(\tau) = \left(\frac{1}{1+\tau/\hat{\tau}_G}\right)\left(\frac{1}{1+(w_r/w_z)^2\tau/\hat{\tau}_G}\right)^{1/2} \qquad (21)$$

where $\hat{\tau}_G = w_r^2/8D$ is usually referred to as a "characteristic" diffusion time [28]. In the case of a Gaussian-Lorentzian profile the solution to $p_{in}(\tau)$ cannot be expressed analytically [29], however an approximation which is good to within a few percent yields

$$p_{in}(\tau) \approx \left(\frac{1}{1+\tau/\hat{\tau}_L}\right)\sqrt{\pi\zeta/\tau}e^{\zeta/\tau}\mathrm{erfc}\left[\sqrt{\zeta/\tau}\right] \qquad (22)$$

where $\zeta = z_0^2/D$ and the "characteristic" diffusion time here is $\hat{\tau}_L = w_r^2/6D$. By substituting the more exact expression for $p_{in}(\tau)$ into equation (16) alongside the appropriate approximation to $g(\tau)$ from equation (18), one can expect to approximate $G_F(\tau)$ reasonably well both for the fast time scales governing molecular internal dynamics and for the slow time scales governing molecular external (diffusional) dynamics. Such an approach has been used previously [30].

It is useful at this point to clarify the difference between the characteristic diffusion times $\hat{\tau}$ listed above and the dwell times listed in Section 4 (Eqs. (11) and (12)). Characteristic times roughly correspond to $p_{in} \approx 1/2$, and hence may be thought of as median autocorrelation times. That is, given a population of molecules in V, roughly half this population will have left V after the characteristic diffusion time. This time should not be confused with the mean autocorrelation time, rigorously defined as $\overline{\tau} = \int_0^\infty p_{in}(\tau)d\tau$, which is longer than $\hat{\tau}$ owing to the slow decay of $p_{in}(\tau)$ (particularly in the case of a Gaussian-Lorentzian profile). The mean autocorrelation times reflect the average duration of molecular trajectories in V given arbitrary starting points on the trajectories. In contrast, the dwell times τ_d as defined by equation (9) reflect the average duration of complete molecular trajectories from the times when molecules first enter V to the times when they last exit V. This difference in definition is not sufficient, in general, to guaranty that $\tau_d > \overline{\tau}$ (for example, τ_d and $\overline{\tau}$ would be equal if $p_{in}(\tau)$ were simply governed by the exponential dynamics of equation (17) (see paradox in [31]). Nonetheless, $\tau_d > \overline{\tau}$ is valid for the $p_{in}(\tau)$ of a Gaussian-ellipsoid profile, and appears to be valid for the exact $p_{in}(\tau)$ of a Gaussian-Lorentzian profile.

In short, the dwell times listed in equations (11) and (12) tend to be significantly longer than the characteristic times listed above.

6 Pulse saturation

Thus far, we have discussed how the fluorescence of molecules depends on the excitation rate constant $\overline{\alpha}$. Referring to equation (1) which defines the average fluorescence generated per molecule, we have seen in particular that $\overline{f}$ varies linearly with $\overline{\alpha}$ only insofar as there is no ground-state depletion. In the event of ground-state depletion, due to ISC or photobleaching for example, then the dependence of $\overline{f}$ on $\overline{\alpha}$ becomes sub-linear. We remind the reader that $\overline{\alpha}$ is a generalized rate constant which in turns depends on the intensity of the illumination beam I. Since I is a parameter which can be readily controlled in experiment, it is important to understand its influence in detail, particularly in the context of pulsed *versus* CW illumination.

Let us first consider the case of CW illumination and define $\overline{\alpha}(\overline{I})$ as the functional dependence of $\overline{\alpha}$ on $\overline{I}$ specifically for this case. In particular, $\overline{\alpha}$ is proportional to $\overline{I}^2$ for 2PE, to $\overline{I}^3$ for 3PE, *etc.* When $\overline{I}$ is increased, then $\overline{\alpha}$ is increased accordingly (to a point – we neglect very high intensity phenomena such as stimulated emission, self-focusing, ionization, *etc.*).

We now consider the case of pulsed illumination, which is almost always necessary for adequate MPE. As discussed in Section 2, $\overline{\alpha}$ is then properly defined as ξ/τ_l, where we recall that ξ represents the probability that a single pulse excites a ground-state molecule. On examining the functional dependence of ξ on $\overline{I}$ (in the regime where $\tau_p \ll \tau_e$; see Sect. 2), we find that when $\overline{I}$ is increased then ξ cannot increase indefinitely since it must be bounded between 0 and 1. Specifically, we find the relation $\xi = 1 - e^{-\overline{\alpha}\tau_l}$ (using Eqs. (A.1-A.3)), or again

$$\hat{\alpha} = \frac{1}{\tau_l}(1 - e^{-\overline{\alpha}\tau_l}) \qquad (23)$$

(for ease of notation, we use a caret to identify the case of pulsed illumination).

Equation (23) indicates that while the time-averaged excitation rate constants for pulsed ($\hat{\alpha}$) and CW ($\overline{\alpha}$) illuminations are equivalent at low intensities, they are manifestly no longer equivalent at high intensities. We refer to the deviation experienced by $\hat{\alpha}$ at high intensities as pulse saturation, since by definition this only applies in the case of pulsed illumination. The onset of pulse saturation occurs at illumination intensities for which $\overline{\alpha}(\overline{I}) \approx 1/\tau_l$, meaning that for popular dyes such as fluorescein or rhodamine and with Ti:Sapphire illumination, the onset of pulse saturation typically occurs at roughly the same intensity as does the onset of ground- state depletion due to intersystem-crossing (see Sect. 3).

We emphasize here that the phenomenon of pulse saturation is a consequence of our having assumed that a molecule can be excited at most only once per pulse, an assumption which is valid for the particular pulse conditions described above. The effect of pulse saturation on the excitation profile is best understood by explicitly separating $\hat{\alpha}$ into amplitude and spatial components, in the same manner as in Appendix B. That is, we write $\hat{\alpha} = \hat{a}\hat{W}(r,z)$, where $\hat{a}$ represents the magnitude of the excitation rate constant at the focal center, and $\hat{W}(r,z)$ represents the spatial profile of the excitation rate constant normalized such that $\hat{W}(0,0) \equiv 1$. From equation (23), we find,

$$\hat{a} = \frac{1}{\tau_l}(1 - e^{-\overline{\alpha}\tau_l}) \qquad (24)$$

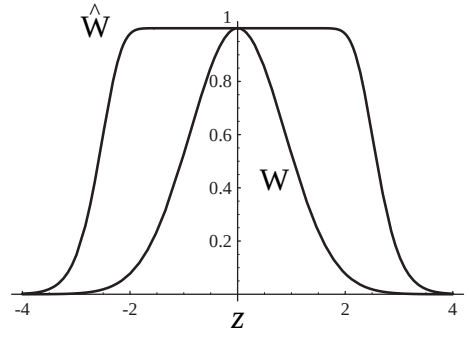

Fig. 6. Normalized profile of 2PE excitation rate constant (along z-axis) in the cases of low- intensity illumination (W = Gaussian-ellipsoid of aspect ratio 1:2.5), and high-intensity illumination ($\hat{W}$).

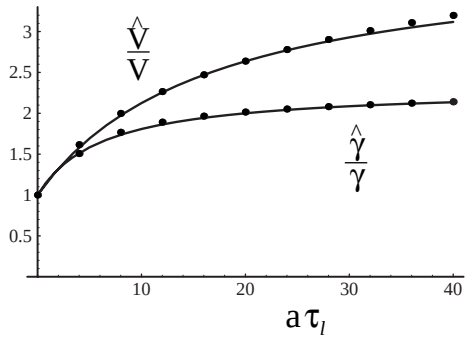

Fig. 7. Effective volume $\hat{V}$ and volume contrast $\hat{\gamma}$ as a function of pulse-saturation parameter $a\tau_l$ characterizing excitation strength (normalized to unsaturated V and γ). Approximations given by equations (28) and (29) (solid lines) are compared to exact results (bullets) for Gaussian-ellipsoid illumination of aspect ratio 1:2.5.

$$\hat{W}(r,z) = \frac{1 - e^{-\overline{a}W(r,z)\tau_l}}{1 - e^{-\overline{a}\tau_l}} \cdot \tag{25}$$

The interpretation of equation (24) is that the magnitude of the excitation rate constant can never exceed the repetition rate of the illumination laser, as expected. The interpretation of equation (25) is illustrated in Figure 6. For small illumination intensities such that $\overline{\alpha}(\overline{I}) \ll 1/\tau_l$, then $\hat{W}(r,z)$ assumes the same unsaturated profile $W(r,z)$ as in the case of CW illumination. However, for large intensities such that $\overline{\alpha}(\overline{I}) \gg 1/\tau_l$, then $\hat{W}(r,z)$ approaches a saturated "top-hat" profile. As in Appendix B, we may assign a volume and contrast parameter to this saturated profile:

$$\hat{V} = \frac{[\int \hat{W}]^2}{\int \hat{W}^2} \tag{26}$$

$$\hat{\gamma} = \frac{\int \hat{W}^2}{\int \hat{W}} \cdot \tag{27}$$

These are illustrated in Figure 7. In general, pulse saturation causes both $\hat{V}$ and $\hat{\gamma}$ to become larger than the corresponding unsaturated V and γ. In particular, $\hat{\gamma}$ approaches 1 for very large illumination intensities, though very slowly. Simple approximations to equations (26) and (27) which are valid in the regime $\overline{\alpha}\tau_l < 40$, which spans most experimental conditions of interest, are given by

$$\hat{V} \approx V\left(\frac{1 + \varepsilon_1 \overline{a}\tau_l}{1 + \varepsilon_2 \overline{a}\tau_l}\right) \tag{28}$$

$$\hat{\gamma} \approx \gamma\left(\frac{1 + \varepsilon_3 \overline{a}\tau_l}{1 + \varepsilon_4 \overline{a}\tau_l}\right) \tag{29}$$

where, for a Gaussian-ellipsoid excitation: $\varepsilon_1 = 0.24$; $\varepsilon_2 = 0.061$, $\varepsilon_3 = 0.37$, $\varepsilon_4 = 0.16$; and for a Gaussian-Lorentzian excitation: $\varepsilon_1 = 0.24$, $\varepsilon_2 = 0.013$, $\varepsilon_3 = 0.45$, $\varepsilon_4 = 0.19$.

We can now gage the effect of pulse saturation on fluorescence emission. Under conditions of no pulse saturation, the fluorescence emitted from a population of molecules is given by equation (6). Under conditions of pulse saturation, equation (6) must be modified. In particular, $\overline{\alpha}$ must be replaced by $\hat{\alpha}$, and C must be replaced by an attendant $\hat{C}$. Following the steps outlined in Section 4 and the general results presented in Appendix C, we approximate $\hat{C}$ as being relatively uniform within the saturated excitation volume $\hat{V}$. The resultant total fluorescence emission (time-averaged) is then finally given by

$$\hat{F} \approx q_r \hat{\gamma} \hat{a} \hat{V} \hat{C}_{in}. \tag{30}$$

Equation (30) is complete in that it takes into account the possibilities of pulse saturation as well as ground-state depletion due to ISC or photobleaching.

Experimental examples of cases where pulse saturation does and does not play a major role in 2PE are illustrated in Figures 8 and 9. In both cases, a same objective (Zeiss water immersion; 40×, NA = 1.2) is used to focus a pulsed Ti:Sapphire laser beam (Spectra-Physics Tsunami; wavelength = 820 nm, $\tau_l = 12$ ns, $\tau_p \approx 200$ fs at sample) into a solution of Rhodamine 6G (R6G) molecules in ultrafiltered Type I water (Barnstead NANOpure). No attempt is made to deoxygenate the water. The resultant fluorescence is epicollected, bandpass filtered, and detected with a photon-counting PMT (Hamamatsu HC125-3). We note that the ratio R, which represents the deviation of the measured 2PE fluorescence from a power-squared law, is independent of the fluorescence detection efficiency.

We have made use of literature values in assigning some photodynamic constants to R6G: $\tau_e \approx 3$ ns [32], $\tau_d \approx 4$ μs [32]; $q_r \approx 0.5$ [33]; $q_{isc} \approx 0.002$ [34]; 2PE action cross-section ≈ 50 GM (this value was measured in methanol [35] and is assumed roughly equivalent in water); average photon yield per molecule before photobleaching $\sim 2.5 \times 10^4$ (yield = q_r/q_b). We note that there is some variance in the literature as to the exact photon-yield of R6G in water, which has been reported to be dependent on wavelength [36] and on illumination intensity [37]. We have chosen here a value which corresponds to the "high-intensity" regime in reference [37] (this reference uses an alternative definition of photon-yield), and corresponds to the reported value [33] based on an approach which fully takes into account illumination beam profile, though perhaps inadequately takes into account ISC at the very focal

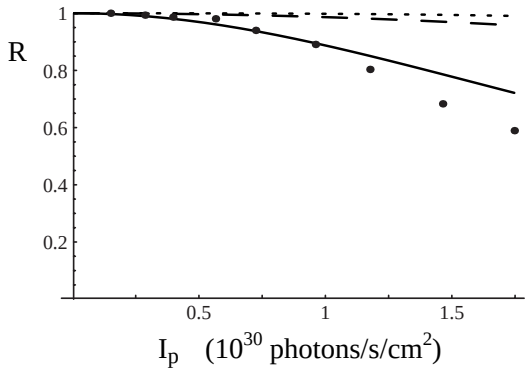

Fig. 8. Steady-state 2PE fluorescence from solution of R6G molecules in water excited with a Gaussian-Lorentzian illumination profile ($w_r = 0.75$ μm). R is the deviation of fluorescence from a power-squared dependence on peak pulse-intensity at the focal center I_p (photons/s/cm^2) due to pulse-saturation alone (dotted), pulse-saturation+ISC (dashed), and pulse-saturation+ISC+photobleaching (solid). Model is compared to experimental results (bullets).

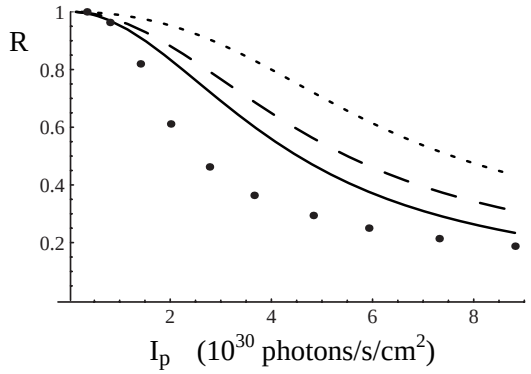

Fig. 9. Steady-state 2PE fluorescence from solution of R6G molecules in water excited with a Gaussian-ellipsoid illumination profile ($w_r = 0.34$ μm; $w_z = 0.8$ μm). R is the deviation of fluorescence from a power-squared dependence on peak pulse-intensity at the focal center I_p (photons/s/cm^2) due to pulse-saturation alone (dotted), pulse-saturation+ISC (dashed), and pulse- saturation+ISC+ photobleaching (solid). Model is compared to experimental results (bullets).

center. Except for the 2PE cross-section, the photophysical constants listed above are all derived from 1PE experiments, and hence can only be *assumed* to apply in the case of 2PE.

In the case of Figure 8, the back aperture of the objective is underfilled by a ratio 1:5, resulting in an approximately Gaussian-Lorentzian illumination profile in the sample ($V \approx 20$ fL, $\tau_d \approx 3$ ms). In the case of Figure 9, the back aperture of the objective is overfilled, resulting in an approximately Gaussian-ellipsoid illumination profile in the sample ($V \approx 0.2$ fL, $\tau_d \approx 0.2$ ms). For a same laser power, the intensity at the sample is about 10 times smaller when the back-aperture is underfilled than when it is overfilled. In the former case, the deviation of fluorescence from a power-squared law is primarily governed by photobleaching while the effects of pulse saturation are negligible. In the latter case, the deviation from a power squared law is primarily governed by pulse saturation while the effects of photobleaching become less prominent. In both cases, as predicted in Section 3 for Ti:Sapphire illumination, the effects of ISC, while not entirely negligible, are distinctly of lesser importance than either photobleaching or pulse saturation. As a rule of thumb, the effects of photobleaching dominate those of pulse saturation when $q_b\tau_d \gg \tau_l$, and *vice-versa*.

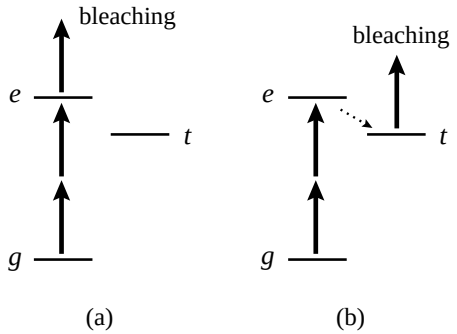

Fig. 10. Possible scenarios for 3PE photobleaching. Molecule is excited to state e by 2PE, and becomes photobleached after absorbing a third photon from state e (a) or state t (b).

7 High-order photobleaching and single-molecule detection

As is evident from Figure 8 and particularly Figure 9, there is a discrepancy between the fluorescence predicted by our model and that observed in experiment, even at modest illumination intensities. We discuss some possible reasons for this discrepancy, since these lead to important consequences in establishing criteria for the possibility of single-molecule detection.

We have tacitly assumed so far that the photobleaching rate constant of a molecule scales in the same manner as the fluorescence rate constant. That is, we have assumed that q_b is effectively a constant independent of the illumination intensity. Such an assumption is commonly accepted *a priori*, though it is rarely justified. Indeed, a recent report [37] indicates that q_b may in fact be intensity dependent for R6G in water under 1-photon absorption. Further experiments involving 2-photon absorption [23, 25] suggest that, at least for certain fluorescent molecules, photobleaching may be governed by processes involving the absorption of 3 photons or more. In this section we generalize our model to include the possibility of such higher order photobleaching processes.

Let us consider, for example, the case where fluorescence is governed by 2PE (*i.e.* $f \propto I^2$), whereas photobleaching is governed by 3PE (*i.e.* $q_b \propto I$). Some possible scenarios for 3PE photobleaching are depicted in Figure 10, involving the absorption of a third photon from the singlet manifold or the triplet manifold. The latter scenario, for example, has been proposed for the photobleaching of Rhodamine B on a glass surface [38]. The

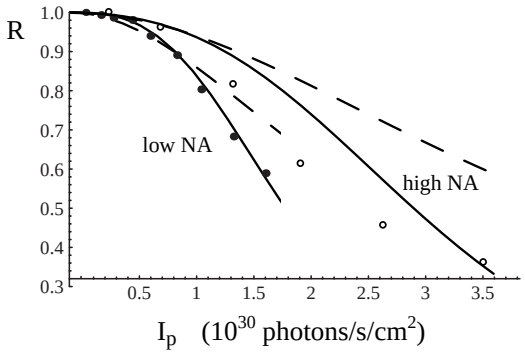

Fig. 11. Comparison of models for steady-state 2PE fluorescence of R6G molecules in water, based on 2PE photobleaching (dashed) or 3PE photobleaching (solid). Excitation configurations are Gaussian-Lorentzian (low NA; see Fig. 8) or Gaussian-ellipsoid (high NA; see Fig. 9). Models are compared to experimental results (bullets).

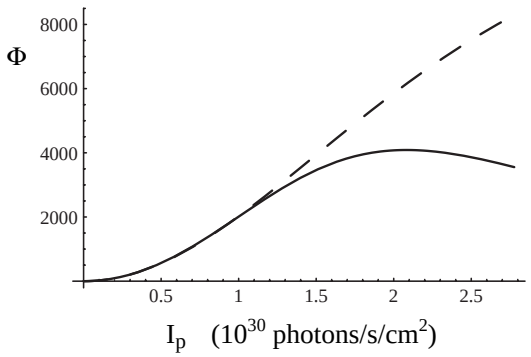

Fig. 12. Expected number of 2PE fluorescence photons generated by a single R6G molecule in water after it enters excitation volume with Gaussian-Lorentzian profile ($w_r = 0.75$ μm). Dashed line includes possibility of 2PE photobleaching. Solid line includes possibility of 3PE photobleaching.

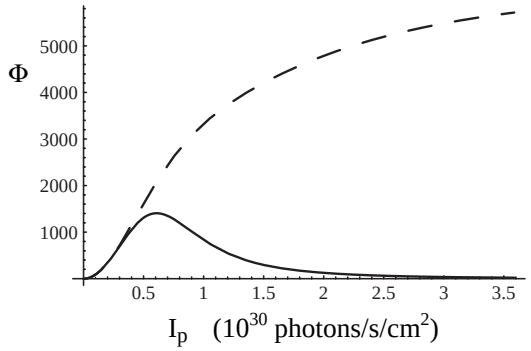

Fig. 13. Expected number of 2PE fluorescence photons generated by a single rhodamine molecule in water after it enters excitation volume with Gaussian-ellipsoid profile ($w_r = 0.34$ μm and $w_z = 0.8$ μm). Dashed line includes possibility of 2PE photobleaching. Solid line includes possibility of 3PE photobleaching.

exact proportionality between q_b and I largely depends in the above cases on the lifetime of the intermediate state from which the third photon is absorbed. We note that it is possible to identify the scenarios depicted in Figure 10 by using FCS with different laser repetition rates (using a pulse picker). This is in contrast to the situation depicted in Figure 5 (constant q_{eb} and/or q_{tb}), where FCS cannot distinguish between photobleaching from the singlet or triplet manifold.

An estimate of the rate constant $\overline{\beta}$ for possible 3-photon photobleaching may be obtained from fits to the experimental results in Figures 8 and 9. For modest peak illumination intensities ($I_p < 3 \times 10^{30}$ photons/s/cm^2), these fits turn out to be considerably more accurate than those provided by a 2-photon photobleaching model (Fig. 11), suggesting that for R6G in water and for the particular excitation conditions described above, photobleaching may indeed be dominated by photon absorption processes of order greater than 2. For very high peak illumination intensities, however, the measured deviation from a power-squared dependence is less than that predicted by our 3PE photobleaching model, and indeed less than that predicted even by our 2PE photobleaching model, suggesting the occurrence of other photophysical processes not taken into account by our model. Similar observations in the case high peak intensities have been reported previously [39], for which the proposed explanation involved stimulated emission from the excited singlet state which moderates the effect of ISC (as well as any photobleaching from the triplet manifold).

In the regime where stimulated emission may be neglected, we illustrate the effects of possible high-order photobleaching by quantifying the amount of fluorescence that can be expected from a single molecule in the excitation volume. Such a quantification is indispensable in establishing the conditions for single molecule detection, that is, the conditions whereby a single molecule can generate more signal photons than background photons, and enough signal photons to allow one to identify the molecule with high confidence.

The average number of photons generated by a single molecule is simply given by:

$$\phi \approx q_r \langle \overline{f} \rangle \tau_{eff} \tag{31}$$

where $\langle \overline{f} \rangle$ is the average fluorescence rate of the molecule while in the excitation volume (defined from Eq. (30)), and τ_{eff} is the average dwell time of the molecule in the excitation volume taking into account the possibility that the molecule may effectively "exit" the volume by photobleaching as well as diffusion (see Eq. (20)). As before, $\langle \overline{f} \rangle$ is governed by the internal dynamics of the molecule, whereas τ_{eff} is governed by the external dynamics of the molecule resulting from its being in an open system.

We use equation (31) to derive the 2PE fluorescence signals one might expect for the detection of single R6G molecules under various conditions. These signals are illustrated in Figures 12 and 13. We note that, in the case of 2-photon photobleaching, then f and β scale identically with the illumination intensity I. One expects, therefore, that as I is increased, then ϕ increases quadratically in the regime $\overline{\beta} \ll 1/\tau_d$ and then begins to plateau when

$\overline{\beta} > 1/\tau_d$. At very high intensities such that a molecule only rarely reaches the focal center without being photobleached (see Appendix C), then ϕ begins to drop again (not shown in Figs.). In the case of 3-photon photobleaching, the ratio f to β scales inversely with I. The peaking in ϕ therefore occurs at much lower illumination intensities. We note that in the case of a tight focus (Fig. 13), 2PE photobleaching plays a relatively minor role because of short diffusional dwell times despite high focal intensities, whereas just the opposite is true for 3PE photobleaching. It is possible that high-order photobleaching may, in fact, be responsible for the experimental difficulties encountered in obtaining high 2PE fluorescence from single molecules.

We must emphasize that we have entirely neglected a possible dependence of photobleaching on excitation wavelength [36], and hence the model we have presented does not constitute a complete or general theory of high-order multi-photon photobleaching. We have also neglected the possibility that q_{isc} may be intensity and/or wavelength dependent. In particular, short excitation wavelengths may promote molecules to higher level excited singlet states, allowing more channels for ISC. Suffice it to say, however, that the results shown above for R6G suggest that there may be cases where photobleaching plays a significant role in limiting fluorescence generation, and that further studies into the exact dynamics of photobleaching for specific molecules under specific excitation conditions are warranted.

8 Conclusion

A touchstone in fluorescence imaging is the ability to detect single molecules in solution. We have presented a simple model based on equation (1) which describes how the multi-photon excited fluorescence rate of molecules, both under CW and pulsed illumination, is proportional to the product of the ground-state population and the excitation rate constant. The purpose of this paper has been to quantify some factors limiting this fluorescence rate. As in the case of 1PE fluorescence, these factors include ground-state depletion due to ISC and photobleaching, though for MPE the qualitative nature of the depletion by photobleaching differs owing to the inherent confinement of the excitation volume in 3-dimensions. In the case of short pulsed illumination, which is characteristic of MPE, a further factor limiting the fluorescence rate of molecules is the saturation of the excitation rate constant which is defined when the time necessary for a molecule to recuperate from an excitation (τ_e) is much longer than duration of the illumination pulse (τ_p). We have adopted a simple model to combine these factors, making use of rigorous definitions of such notions as excitation volume, volume contrast, and diffusion dwell times. Qualitative observations suggest that the photobleaching constant for R6G in water for 2PE increases at least linearly with intensity.

Most of the theoretical work and all the experimental work for this article were carried in the group of W.W. Webb at Cornell University, funded by the NSF (grant BIR8800278) and the NIH (grants RR04224 and RR07719). The author is grateful to Prof. Webb for his support and fruitful discussions. Additional thanks go out to C. Xu, E. Brown, M. Albota, L. Moreaux, W. Zipfel, R. Williams and H. Stone.

Appendix A

In this appendix, we define what is meant by the characteristic pulse width of an excitation beam used in MPE. The most commonly used definition of pulse width is given by the full width at half maximum (FWHM) of the pulse profile, or $\tau_{1/2}$, assumed identical for each pulse. This width may be measured experimentally using an optical autocorrelator, however such a measurement presupposes an *a priori* knowledge of the pulse shape. We will adopt an alternative definition of pulse width which does not presuppose such an *a priori* knowledge, and which is more convenient to use in the context of MPE.

We denote n as the MPE order, that is, $n = 2$ for 2PE, $n = 3$ for 3PE, *etc.* The relevant n-th order autocorrelation factor of the excitation beam, which is sometimes referred to as the pulsed beam "advantage factor", is defined as [40]

$$g_n = \frac{\overline{I^n}}{\overline{I}^n} \tag{A.1}$$

where I is the excitation beam intensity and the overstrike denotes a long time average. We define the characteristic pulse width τ_p of the excitation beam through the simple relation

$$g_n = \left(\frac{\tau_l}{\tau_p}\right)^{n-1} \tag{A.2}$$

where τ_l is the pulse period (*i.e.* the inverse repetition rate of the excitation beam). Similarly, we define the characteristic pulse intensity I_p of the excitation beam through the relation

$$g_n = \left(\frac{I_p}{\overline{I}}\right)^{n-1} \tag{A.3}$$

(or equivalently $I_p = \overline{I}\tau_l/\tau_p$; see Fig. 14). In other words, rather than basing the definitions of τ_p and I_p on pulse shape, which is difficult to measure and must usually be assumed, we base our definitions directly on g_n, which is the parameter of relevance in MPE. In the case of 2PE, g_2 can be measured with a standard optical autocorrelator using the 2nd harmonic generation from a nonlinear crystal. Alternatively, g_2 can be measured *in situ* from the sample produced fluorescence, with or without a knowledge of the absolute 2PE cross-section of the sample [41]. This latter technique may also be used to measure g_n's of higher order than 2.

For reference purposes, we relate the characteristic pulse width τ_p to the full-width half-maximum time $\tau_{1/2}$.

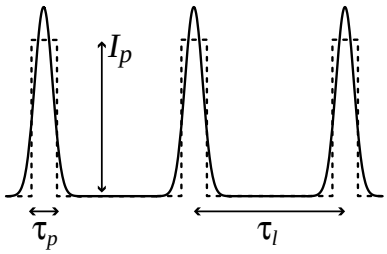

Fig. 14. True pulse train (solid) and corresponding "top-hat" pulse train (dashed) possess identical MPE properties.

In the case of a Gaussian pulse profile, $\tau_p = 1.52\tau_{1/2}$ for $n = 2$, $\tau_p = 1.40\tau_{1/2}$ for $n = 3$, *etc.* In the case of a Sech^2 profile, $\tau_p = 1.69\tau_{1/2}$ for $n = 2$, $\tau_p = 1.56\tau_{1/2}$ for $n = 3$, *etc.*

Appendix B

Throughout the literature, a number of definitions have been proposed for quantifying the excitation volume for MPE. Typically, these definitions rely on assigning a ratio between the amount of MPE fluorescence generated inside the volume *versus* the amount of fluorescence generated outside the volume. Since there is little justification in choosing one particular ratio over another, these definitions are fundamentally arbitrary.

In this appendix, we derive a rigorous definition of what is meant by the excitation volume for MPE of any order. The definition is based on a derivation of the *number* of molecules inside the excitation volume [23], where we specify here that we regard a molecule as a well defined entity independently of its internal state (for example, a molecule remains the same molecule even if it becomes photobleached).

Let us first consider the number of molecules inside an arbitrary volume (assumed much smaller than the sample volume). In the case when the molecules are diffusing freely, then their motion is Brownian. That is, the number of molecules $N(t)$ in the volume at any given time t is subject to Poissonian statistics: the variance in $N(t)$ is equal to the time-averaged number of molecules in the volume $\overline{N}$. In terms of the normalized auto-correlation factor of the number fluctuations $\delta N(t) = N(t) - \overline{N}$ (see Sect. 5), we find therefore

$$G_N(0) = \frac{1}{\overline{N}} \cdot \tag{B.1}$$

The above relation applies to an arbitrary volume. We are specifically interested, however, in the volume that encompasses only the molecules that are excited by the incident illumination beam. We identify these molecules by the instantaneous fluorescence they produce, which is given by

$$F(t) = q_r \int \alpha(\mathbf{x}, t) C(\mathbf{x}, t) dv \tag{B.2}$$

where q_r is the radiative quantum yield, $\alpha(\mathbf{x}, t)$ is the local excitation rate constant, $C(\mathbf{x}, t)$ is the local molecular concentration, and the integration is over the entire sample volume (assumed large). Strictly speaking, C above represents the concentration of *excitable* molecules, however because we do not wish here to distinguish between excitable and non-excitable molecules, we place ourselves in the limit where every molecule may be considered excitable. That is, we discount the possibility of ground-state depletion due to ISC or photobleaching, or equivalently, we assume that the illumination intensity is low.

Let us consider only those fluctuations that occur over time scales longer than the excited state lifetime τ_e and longer than the interval τ_l between illumination pulses, that is, let us consider fluctuations whose durations are at least of order hundreds of nanoseconds or greater. We can write then

$$\delta F(t) = q_r \int \overline{\alpha}(\mathbf{x}) \delta C(\mathbf{x}, t) dv \tag{B.3}$$

where the precise meaning of $\overline{\alpha}$ is detailed in Section 2. The fluctuations $\delta F(t)$ are directly related here to the fluctuations $\delta C(\mathbf{x}, t)$, and hence, in the limit where molecular internal dynamics are neglected, reflect only the diffusional dynamics of the illuminated molecules. As such, we can make the direct correspondence $G_F(\tau) \equiv G_N(\tau)$. We find therefore, in the small time limit [42],

$$G_F(0_+) = \frac{1}{\overline{N}} \cdot \tag{B.4}$$

Equation (B.4) provides an unambiguous definition of the average number of molecules $\overline{N}$ that can be excited by an illumination beam of arbitrary profile. Through the simple relation $\overline{N} = \overline{C}V$, equation (B.4) provides therefore an unambiguous definition of the excitation volume V.

The final step in formulating V requires an analytic expression for $G_F(0_+)$. This is given by [18]

$$G_F(0_+) = \frac{\int \overline{\alpha}(\mathbf{x})^2 dv}{\overline{C}[\int \overline{\alpha}(\mathbf{x}) dv]^2} \cdot \tag{B.5}$$

which depends on the illumination beam profile. Writing $\overline{\alpha}(\mathbf{x}) = aW(\mathbf{x})$ where $a = \overline{\alpha}(0)$ is the excitation amplitude exactly at the illumination beam focal center, and $W(\mathbf{x})$ is the unitless normalized excitation profile ($W(0) = 1$), and combining equations (B.4) and (B.5), we finally arrive at

$$V = \gamma^{-1} \int W(\mathbf{x}) dv \tag{B.6}$$

where we have introduced the concept of a volume contrast, defined by

$$\gamma = \frac{\int W(\mathbf{x})^2 dv}{\int W(\mathbf{x}) dv} \tag{B.7}$$

to characterize the sharpness of the volume boundaries. γ varies between 0 and 1, where $\gamma = 1$ characterizes a "top-hat" volume with perfectly sharp boundaries. Defining

$\langle\overline{\alpha}\rangle = \overline{F}/q_r\overline{N}$ as the average excitation rate of a molecule in V, we find $\langle\overline{\alpha}\rangle = \gamma a$.

We have purposefully kept the intensity dependence of $\alpha(\mathbf{x})$ arbitrary in equation (B.5), though we remind the reader that $\alpha(\mathbf{x})$ (and hence $W(\mathbf{x})$) is proportional $I(\mathbf{x})^n$, where n is the MPE order. For the case of a Gaussian-ellipsoid illumination profile, which is a good approximation when focusing with a high NA objective and overfilling the back aperture, then

$$I(\mathbf{x}) = I(0)e^{-2r^2/w_r^2}e^{-2z^2/w_z^2} \tag{B.8}$$

where w_r and w_z are the radial and axial waists of the profile. Hence $V = (\pi/n)^{3/2}w_r^2 w_z$, and $\gamma = 1/\sqrt{8}$ regardless of n. Numerical fits for NA > 0.8 and $n \geq 2$ yield $w_r \approx 0.52\lambda/\sin\theta$ and $w_z \approx 0.76\lambda/(1-\cos\theta)$, where λ is the wavelength of the illumination beam in the sample and θ is the half-angle spanned by the illumination beam in the sample [43].

For the case of a Gaussian-Lorentzian illumination profile, which is a good approximation when underfilling the back aperture, then

$$I(\mathbf{x}) = I(0)(w_r^2/w^2(z))e^{-2r^2/w^2(z)} \tag{B.9}$$

where $w^2(z) = w_r^2(1 + z^2/z_0^2)$ and $z_0 = \pi w_r^2/\lambda$ is the Rayleigh length. In this case, $V = (4/3)\pi^2 w_r^2 z_0$ and $\gamma = 3/16$ when $n = 2$, and $V = (32/105)\pi^2 w_r^2 z_0$ and $\gamma = 35/128$ when $n = 3$, *etc.*

Finally, we call to attention the similarities in the definitions for the excitation volume V (Eq. (B.5)) and the excitation pulse width τ_p (defined through Eqs. (A.1) and (A.2)), which, aside from a difference in units, are qualitatively identical.

Appendix C

We present an exact solution to equation (5) for the case of a "hard-sphere" excitation volume. Though such a volume is unrealizable in practice, it provides significant insight into the behavior of equation (5) for more general excitation volumes, and corroborates the results obtained in Section 4.

To begin, let us consider some general features of a solution to equation (5). Such a solution is governed by diffusion dynamics, meaning that molecular flow rates (*i.e.* concentration gradients) are diffusion limited. In particular this means that, in 3-dimensions, the concentration depletion $[C_\infty - C(r)]$ can vary no faster than of order $\sim 1/r$ about a localized sink. Because photobleaching *via* MPE plays a similar role to that of a localized sink, then we may conclude that as long as the excitation profile $\alpha(r)$ decays faster than $\sim 1/r$ about a focal center, which it must in order to be confined, then the excitation profile will always be narrower than the profile of the resultant concentration depletion. In other words, we may safely assume that $C(r)$ is relatively flat over the dimensions of the excitation profile, as was done in Section 4.

We turn now to the specific case of an excitation profile defined by a hard sphere:

$$\alpha(r) = \begin{cases} a & (r \leq r_0) \\ 0 & (r > r_0). \end{cases} \tag{C.1}$$

That is, the excitation rate constant, and hence the photobleaching rate constant, is a fixed value within a radius r_0 and zero outside this radius. The steady-state solution to equation (5) is analytic, and is given by

$$C(r) = \begin{cases} C_\infty \dfrac{\sinh\kappa r}{\kappa r \cosh\kappa r_0} & (r \leq r_0) \\ C_\infty\left(1 - \dfrac{\kappa r_0 - \tanh\kappa r_0}{\kappa r}\right) & (r > r_0) \end{cases} \tag{C.2}$$

where $\kappa = \sqrt{q_b a/D}$. Several features of this solution are of note. First of all, q_b, a and D enter the solution only through the parameter κ (this is true for solutions to Eq. (5) in general). That is, variations in q_b or a or in the inverse of D are equivalent. Secondly, the concentration depletion varies as $\sim 1/r$ outside the excitation volume, as expected for a general solution to equation (5). Thirdly, upon examining the solution at the focal center $C(0)$ and performing an expansion of $\cosh\kappa r_0$, one may readily identify three regimes: i) if $\kappa r_0 < 0.1$ then $C(0)/C_\infty \approx 1$, meaning that there is essentially no concentration depletion, ii) if $0.1 < \kappa r_0 < 3$ then depletion occurs such that the depletion depth $C(0)/C_\infty$ scales as $1/\kappa r_0$ whereas the depletion width remains relatively constant, and finally iii) if $\kappa r_0 > 3$ the depletion becomes saturated, that is, $C(0)/C_\infty$ scales as a higher power of $1/\kappa r_0$ and the depletion width begins to grow. The first two regimes i) and ii) are almost identically described by the linear approximation equation (8) for the average concentration in the excitation volume, and basically define the regimes for which equation (8) is valid. In both these regimes, though depletion may occur, the probability that molecules can diffuse to the focal center of the excitation volume remains significant. On the other hand, in regime iii), then $C(0)$ is close to zero meaning that $\nabla^2 C|_{r=0} \approx 0$. The probability that a molecule from outside the excitation volume can diffuse all the way to the focal center without being photobleached becomes negligible here. In this regime, molecular fluorescence is generated primarily from the fringes of the excitation volume.

Although our separation of the steady-state depletion solution into three regimes has been applied to the specific case of a hard-sphere excitation volume, it is generally valid for any shape of excitation volume confined in 3-dimensions. For a spherically symmetric volume, the quantity r_0 should be regarded as the characteristic radius of the volume. For a cylindrically symmetric volume, as is usually encountered in practice, the quantity r_0 should be regarded as closer to the radial dimension than to the (longer) axial dimension of the volume, the reason being that the dwell times of molecules in the volume are primarily governed by the radial dimension (see Eqs. (11) and (12)).

References

1. J.B. Pawley, *Handbook of Biological Confocal Microscopy* (Plenum Press, New York, 1995).
2. W. Denk, J.H. Strickler, W.W. Webb, Sci. **248**, 73-76 (1990).
3. C. Xu, W.W. Webb, J. Opt. Soc. Am. B **13**, 481-491 (1996).
4. C. Xu, W. Zipfel, R. Williams, W.W. Webb, Proc. Natl. Acad. Sci. (USA) **93**, 10763-10768 (1996).
5. S.W. Hell, K. Bahlmann, M. Schrader, A. Soini, H. Malak, I. Gryczynski, J.R. Lakowicz, J. Med. Opt. **1**, 71-74 (1996).
6. D.L. Wokosin, V.E. Centoze, S. Crittenden, J. White, Bioimaging **4**, 1-7 (1996).
7. E.H.K. Stelzer, S. Hell, S. Lindek, Opt. Commun. **104**, 223-228 (1994).
8. R.M. Williams, D.W. Piston, W.W. Webb, FASEB J. **8**, 804-813 (1994).
9. W. Denk, K.R. Delaney, A. Gelperin, D. Kleinfeld, B.W. Strowbridge, D.W. Tank, R. Yuste, J. Neuro. Meth. **54**, 151-162 (1994).
10. K. Svoboda, W. Denk, D. Kleinfeld, D.W. Tank, Nature **385**, 161-165 (1997).
11. D.W. Piston, B.R. Masters, W.W. Webb, J. Microsc. **178**, 20-27 (1995).
12. S. Potter, C.-M. Wang, P. Garrity, S. Fraser, Gene **173**, 25-31 (1996).
13. K.D. Niswender, S.M. Blackman, L. Rohde, *et al.*, J. Microsc. **180**, 109-116 (1995).
14. J.B. Shear, E.B. Brown, W.W. Webb, Anal. Chem. **68**, 1778-1783 (1996).
15. S. Maiti, J. Shear, R. Williams, *et al.*, Sci. **275**, 530-532 (1997).
16. D. Magde, E.L. Elson, W.W. Webb, Phys. Rev. Lett. **29**, 705-708 (1972).
17. R. Rigler, J. Widengren, U. Mets, in *Fluorescence spectroscopy: new methods and applications*, edited by O.S. Wolfbeis (Springer, Berlin, 1992), pp. 13-24.
18. N.L. Thompson, "*Fluorescence correlation spectroscopy*," in *Topics in fluorescence spectroscopy, Vol. 1: techniques*, edited by J.R. Lakowicz (Plenum, New York, 1991), pp. 337-378.
19. S. Maiti, U. Haupts, W.W. Webb, Proc. Natl. Acad. Sci. (USA) **94**, 11753-11757 (1997).
20. D. Axelrod, D.E. Koppel, J. Schlessinger, E. Elson, W.W. Webb, Biophys. J. **16**, 1055-1069 (1976).
21. W. Denk, Proc. Natl. Acad. Sci. (USA) **91**, 6629-6633 (1994).
22. P. Lipp, C. Luescher, C. Amstutz, E. Niggli, in *Artificial CA spark by diffraction-limited two-photon photolysis*, presented at the 41st annual meeting of the Biophysical Society, New Orleans, 1997 (unpublished).
23. J. Mertz, C. Xu, W.W. Webb, Opt. Lett. 2532-2534 (1995).
24. K. Berland, P.T.C. So, E. Gratton, in *Fluorescence detection of single molecules by two-photon excitation*, presented at the 40th annual meeting of the Biophysical Society, Baltimore, 1996 (unpublished).
25. L. Brand, C. Eggeling, C. Zander, K.H. Drexhage, C.A.M. Seidel, J. Phys. Chem. A **101**, 4313-4321 (1997).
26. W.H. Press, S.A. Teukolsky, W.T. Vetterling, B.P. Flannery, *Numerical recipes in C* (Cambridge University Press, Cambridge, 1992).
27. H.C. Berg, *Random walks in biology* (Princeton University Press, Princeton, 1993).
28. M. Eigen, R. Rigler, Proc. Natl. Acad. Sci. (USA) **91**, 5740 (1994).
29. K.M. Berland, P.T.C. So, E. Gratton, Biophys. J. **68**, 694-701 (1995).
30. J. Widengren, U. Mets, R. Rigler, J. Phys. Chem. **99**, 13368-13378 (1995).
31. N.G. van Kampen, *Stochastic processes in physics and chemistry* (North-Holland, Amsterdam, 1981), p. 51.
32. Z. Zander, M. Sauer, K.H. Drexhage, D.-S. Ko, A. Schulz, J. Wolfrum, L. Brand, C. Eggeling, C.A.M. Seidel, Appl. Phys. B **63**, 517-523 (1996).
33. S.A. Soper, H.L. Nutter, R.A. Keller, L.M. Davis, E. Brooks Shera, Photochem. Photobiol. **57**, 972-977 (1993).
34. M.M. Asimov, V.N. Gavrilenko, A.N. Rubinov, J. Lumin. **46**, 243-249 (1990).
35. M. Albota, C. Xu, W.W. Webb, Appl. Opt. (to be published).
36. A.V. Aristov, Opt. Spect. **77**, 856-857 (1994).
37. J. Widengren, R. Rigler, Bioimaging **4**, 149-157 (1996).
38. E.J. Sanchez, L. Novotny, G.R. Holtom, S.X. Xie, J. Phys. Chem. A **101**, 7019-703 (1997).
39. J.P. Hermann, J. Ducuing, Opt. Comm. **6**, 101-105 (1972).
40. R. Loudon, *The quantum theory of light* (Oxford University Press, Oxford, 1983).
41. C. Xu, J. Guild, W.W. Webb, *et al.*, Opt. Lett. **20**, 2372-2374 (1995).
42. The time $\tau = 0_+$ is small relative to diffusional time scales, but still large relative to τ_l or τ_e; hence, the fluctuations arising from the pulsed nature of the illumination beam or from fluorescence anti-bunching are not included in $C_F(0_+)$, nor is shot-noise which is only manifest at $\tau = 0$.
43. C.J.R. Sheppard, H.J. Mattheus, J. Opt. Soc. Am. A **4**, 1354-1360 (1987).